Sciences, Technologies et Développement, volume 23, pp1-13, Novembre 2021

http://www.univ-douala.com/std/

ISSN 1029 – 2225 – e-ISSN 2313-6278

Paleostresses and Kinematic markers analysis from the Garoua basin (North Cameroon, Central Africa): Implications for the tectonic reconstitution

Etoundi Akoa philémon Rémi[1], Mvondo Owono François [2*], Ntsama Atangana Jacqueline[3], Ganwa Alembert Alexandre[1], Owona Sébastien[2], Yene Atangana Joseph Quentin[3]

[1]*Department of Earth Sciences, Faculty of Science, University of Ngaounderé, P.O. Box: 454 Ngaounderé, Cameroon*

[2]*Department of Earth Sciences, Faculty of Science, University of Douala, P.O. Box 24157 Douala, Cameroon*

[3]*Department of Earth Sciences, Faculty of Science, University of Yaoundé, P.O. Box 812 Yaoundé, Cameroon*

Received : April 2021 Revised : June 2021 Accepted: July 2021 available online : July 2021

Abstract

The Garoua basin between is one of the Northern Cameroon intracratonic basins. It is located inside the Yola Branch, one of the two branches of the Benue Through. Set up in the Cretaceous during the opening of the South Atlantic, this basin bas been filled mostly by sandstone. These rocks were significantly affected during the post-rift period by multiform and multidirectional fractures. Tectonic analysis based on the paleostresses reconstitution resulting from field data (joints and faults) and combined with literature data were used to constrain the kinematics and the chronology of this deformation. These data show that, during its post-rift phase, the Garoua basin was subjected to a progressive brittle deformation. The values of the stress ration R (0.06 – 1) and stress index R' (1 – 1.94) for tectonic joints and those of faults with R = R' (0.09 – 0.99) show that two tectonic regimes were succeeded in the basin: a strike slip and an extensive regimes. The strike slip regime which occurred first was implemented in two directions: the NW-SE direction (Upper Eocene/Base Oligocene) and the N-S direction (Upper Oligocene). The extensive regime was also implemented in two directions: the NW-SE direction (Lower Miocene) and the NNW-SSE direction (Messinian). The Cameroon Volcanic Line and the Benue Triple Junction seem to be the main geological features that controlled this deformation.

ISSN 1029 – 2225c2016 Sciences, Technologies et Développement

***Key words**: Garoua basin, stress ratio, tectonic regime, Benue Trough, Cameroon*

1. Introduction

Both the genesis and evolution of a basin are controlled by tectonics, sediment flow and eustatism (Homewood, 1992; Youri and Merzeraud, 2005). For intracratonic basins, this evolution largely depends to the tectonic activity degree or reactivations of the geological structures that cross or border the basin. The Garoua intracratonic basin (Fig. 1) located inside the Yola Branch, one of the two branches of the Benue Through was set up in the Cretaceous during the opening of the South Atlantic (Dumont, 1987; Benkhelil, 1988). This basin includes sandstones, conglomerates, siltites and argillites dated Cretaceous to Coniacian (Ntsama, 2013; Bessong et al., 2018). These formations show a very significant deployment of multiform and multidirectional fractures occurred progressively with time. These deformations of different ages cannot be attributed to a single phase of deformation no more in a particular tectonic regime. It is also very difficult to date these deformations because there are not solid structural or petrographic constraints on the field. No real study related to the Kinematic or tectonic evolution of this basin is available.

Therefore this study aims to reconstitute the kinematics and the chronology and document the origin of such a complex fracturing network which affected the basin since its formation in the Cretaceous. Our hypothesis is that the reactivations of the faults bundles which constitute the Benue Triple Junction (BTJ; Maurin et al., 1986; Maurin and Guiraud, 1990; Guiraud and Maurin, 1991; Benkhelil 1988; Wilson and Guiraud, 1992), the several reactivations of the Cameroon Centre Shear Zone (CCSZ; Toteu et al., 2004; Daouda, 2014) and the activity of the Cameroon Volcanic Line (LVC; Ngounouno, 1997; Montigny et al., 2004) have had a significant control on this basin. Our first objective is to characterize the brittle deformation structures i.e. their geometries and spatial organization or attitudes. The second objective is focused on the spatial distribution of paleostresses as well as the tectonic regimes which have succeeded one another. Finally, the third objective is to propose a model of evolution of the basin integrating the contribution of the regional geological structures.

Fractures being the excellent tools for paleostresses especially and tectonic reconstruction evolution of a region (Faure, 1995; Sanderson et al., 2018; Bao et al., 2019) were used document the kinematics of this basin. We applied the dihedral method (Angelier, 1984, 1990; Carey and Brunier, 1974; Etchecopar et al., 1981). The efficiency for the determination of the directions of paleostresses and the prevailing tectonic regime of this approach has been strongly documented (Faure, 1995; Mvondo, 2001).

2. Geological setting

The Garoua intracratonic basin is part of the Yola Branch of the Benue Trough (Fig. 1).This trough of approximately 1000 km long and 100 km wide is an aborted ridge- ridge-ridge triple junction called Benue Triple Junction. It was formed on the Neoproterozoic basement emplaced during the Pan-African orogeny (650–540 Ma) as result of the collision between Congo, Saharan and West African shields (Nzenti et al., 1988; Abdelsalam et al., 2002) during the opening of the Gulf of Guinea in the lower Cretaceous. This basement includes neoproterozoic metasedimentary rocks and pre-, syn- and post-tectonic granitoids (Figs. 1c and 1d; Toteu et al., 1987, 2001, 2004; Penaye et al., 2006; Daouda Dawaï, 2014). These rocks recorded D1 – D3 deformation phases (Toteu et al., 1987; 1990; 2004). D1 characterized by horizontal foliation, isoclinal folds and N110E-N140E stretch lineation.

Corresponding author address: +237696691543 E-mail address: francois_mvondo@hotmail.com

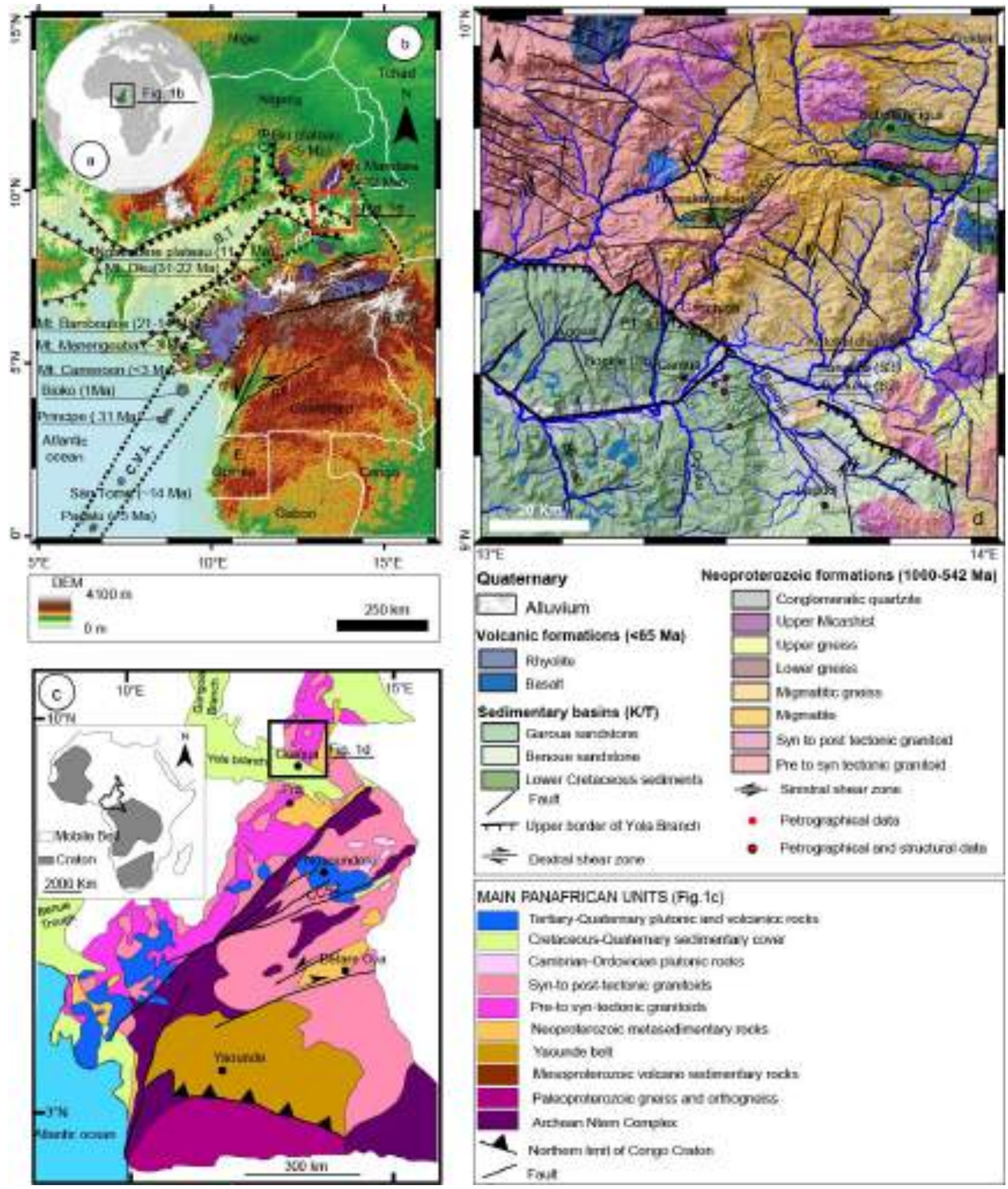

Figure 1. Location maps. **(a)** Cameroon and Africa in the world map, **(b)** Main active geological features crosscutting the Cameroon landform surface and their relationship with the study area, **(c)** Geological map of Cameroon showing the main pan African units (Modified after Toteu et al., 2001; Owona et al., 2012), **(d)** Geological map of the study area. BT: Benue Trough; GB: Gongola Branch; YB: Yola Branch; CVL: Cameroon Volcanic Line; CCSZ: Cameroon Central Shear Zone; SF: Sanaga Faul

D2, characterized by tight folds, vertical axial planes of foliation, mineral lineation parallel to the fold axes oriented NNE-SSW and dipping North or South from 0 to 50 and shears planes. D3 is essentially brittle.

The Garoua basin as the Benue Through was setup during the breakup of the Gondwana, which led to the opening of South Atlantic Ocean at the end of Jurassic-low Cretaceous (Tiessen et al., 1979). It includes conglomerate, sandstone, siltstone and argillite marked by oblique stratifications; parallel laminations and channels characterizing a fluvial environment (Guiraud and Maurin 1991; Bessong et al., 2011; Bessong, 2012; Bessong et al., 2018). These rocks were correlated with the Middle Nigerian Bima Formation (Bessong et al., 2011; Bessong, 2012; Bessong et al., 2018) of Aptian-Albian age (Fig. 2a).

The study area is cross cut and surrounded by the CVL, the CCSZ and the BTJ, three main geological features still active (Popoff et al., 1983; Dumont, 1987; Ngako et al., 1991, 2003).

Three volcanoes of the CVL bordering the study area were iteratively active: to the South, the Adamaoua horst which produced effusive rocks dated 11-7 Ma, to the North, the mounts Mandara made up of volcanic rocks of 32 Ma age and to the West, the Benue Valley whose rocks were dated 37 Ma (Fig. 1; Fitton and Dunlop, 1985; Ngounouno, et al. 1997; Montigny et al., 2004; Deruelle et al., 2007). The Adamaoua horst is crossed by the CCSZ which is a N70E regional ductile

fault having controlled the geometry of the pan- African fold belt in Cameroon. The CCSZ extends from Sudan to NE Brazil (Guiraud et al. 1987; Ngako et al. 2003; Bella Nké et al. 2018). During the late Pan-African tectonic evolution, CCSZ was dextrally reactivated (Ngako et al. 1991). According to Dumont (1987), the CCSZ was also reactivated during the Cretaceous. The NW-SE and late-Cretaceous sub-meridian transpression of the CCSZ would have contributed to the uplift of the Adamaoua massif forming the Adamaoua horst (Benkhelil, 1982).

The BTJ corresponds to the confluence of three rift systems (Fig. 1c): the NE–SW system corresponding to the Benue trough, the E–W system which has evolved to the Central Atlantic margins and the N–S system which has evolved the South Atlantic margins (Benkhelil and Robineau 1983; Guiraud 1991; Benkhelil 1988;Benkhelil 1998). The fault networks that constitute the BTJ are inherited from the Pan-African orogeny and have been frequently reactivated over time (Ambraseys and Adams 1986; Untemehr and Bouche 1986; Ambeh et al. 1988; Benkhelil 1988; Guiraud 1991). Two main reactivations of the BTJ were well recorded: the reverse strike slip play of the N-S and E-W systems and the extensional reactivation of the NE–SW System during the lower Miocene (Benkhelil 1988; Guiraud 1991) and the collapse play of N-S system and the dextral slide E-W and NE–SW systems during the Messinian (Ambraseys and Adams, 1986; Untemehr and Bouche, 1986; Ambeh et al., 1988).

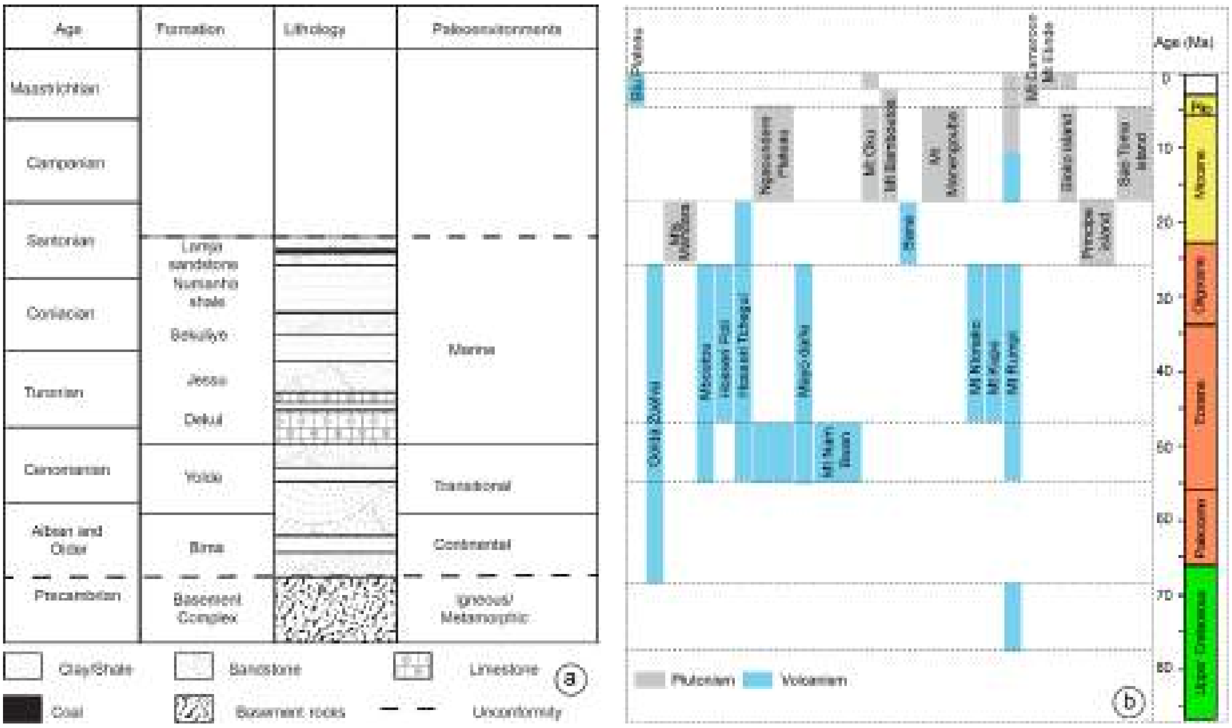

Figure 2. (a) Lithostratigraphic column of the Benue Trough (Abubakar, 2006); **(b)** Histrory of the Cameroon Volcanic Line activity (Kamdem et al., 2002; Déruelle et al., 2007; Moudi et al., 2007; Kamgang et al., 2008; Nkouathio et al., 2008)

3. Data and methodology

This study is mainly based on field data collected from 5 stations: Pitoa (S1), Beckele (S2), Sanguere (S3), Katchatchia (S4) and Bockle (S5) (Fig. 1d). They consist of rocks samples and structural features namely faults and joints attitudes. A total of 178 fault attitudes, 1161 joint attitudes and 567 conjugate structures were identified, described and measured in the field.

The acute dihedral method (Arthaud, 1969; Carey and Brunier, 1974; Etchecopar et al., 1981; Angeler, 1984, 1990; Faure, 1995 and Mvondo, 2001) whose principle consists of the deduction of the stress tensors was used to obtain the orientation of the three principal stresses axes σ_1, σ_2 and σ_3 with $\sigma_1 \geq \sigma_2 \geq \sigma_3$. Indeed, according to this method, the intersection of two planes P_1 and P_2 corresponds to the intermediate principal stress σ_2 while, σ_1 passes through the bisector formed by P_1 and P_2 and belongs to the plane formed by the pole σ_2 passing through σ_3. According to the Mohr circle, three angles are used to describe the distribution of the poles in the case of the filled fractures (Jolly and Sanderson,1997): θ_1 is the angle between the $\sigma2$ stress axis and the border of the fracture pole distribution in the $\sigma2$ - $\sigma3$ plane; θ_2 is the angle between the $\sigma1$ stress axis and the border of the fracture pole distribution in the $\sigma1$- $\sigma3$ plane, and θ_3 is the angle between the $\sigma1$ stress axis and the border of the fracture pole distribution in the $\sigma1$- $\sigma2$ plane. Using these angles, we calculate two parameters: the stress ratio R and the stress index R' to determine the nature of the tectonic regime that prevailed as well as the nature of stress ellipsoid (Faure, 1995; Delvaux et al., 1997; Sanderson et al., 2018). The following equations of Jolly and Sanderson (1997) and Delvaux et al. (1997) were used. According to Jolly and Sanderson (1997), the stress ratio R is a function of the θ_2 and θ_1 angles for and of the θ_2 and θ_3 angles for Pf $>\sigma2$:

- $R = [(1+\cos2\theta_2)/(1+\cos2\theta_1)]$ **(1)** if $Pf < \sigma2$ and
- $R = [1-(1-\cos2\theta_2)/(1-\cos2\theta_3)]$ **(2)** if $Pf > \sigma2$

The term stress regime is used to define the type of stress tensor. The stress regime is determined by the nature of the vertical stress axes: extensional, when σ1 is vertical; strike-slip, when σ2 is vertical; and compressional, when σ3 is vertical. The stress regimes is also a function of the stress ratio R (Table 1; Delvaux et al., 1997): radial extension (σ1 vertical, $0 < R < 0.25$), pure extension (σ1 vertical, $0.25 < R < 0.75$), transtension (σ1 vertical, $0.75 < R < 1$ or σ2 vertical, $1 > R > 0.75$), pure strike-slip (σ2 vertical, $0.75 > R > 0.25$), transpression (σ2 vertical, $0.25 > R > 0$ or σ3 vertical, $0 < R < 0.25$), pure compression (σ3, vertical, $0.25 < R < 0.75$) and radial compression (σ1 vertical, $0.75 < R < 1$). The type of stress regime can be expressed numerically using stress index *R′*, ranging from 0.0 to 3.0 and defined as follows (Table 1):

- $R' = R$ **(3)** when σ1 is vertical (extensional stress regime)
- $R' = 2 - R$ **(4)** when σ2 is vertical (strike-slip stress regime)
- $R' = 2 + R$ **(5)** when σ3 is vertical (compressional stress regime)

The Schmidt canvas, lower hemisphere, was used for the various diagrams. The rose, stereogram, pole and density diagrams were produced via stereonet software.

Table 1. Thresholds values and illustration of the meaning of stress regime index R' versus stress ratio R and orientation of the principal axes of the stress ellipsoid (Delvaux et al., 1997).

Stress tensor type			Extensive				Strike-Slip				Compressive		

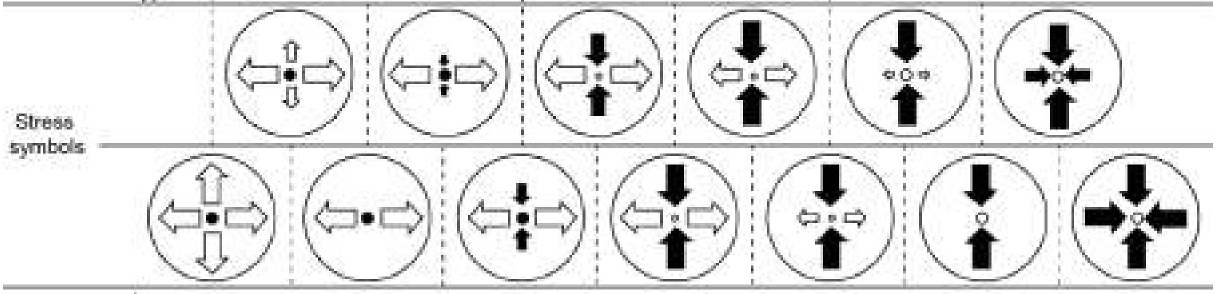

Stress Ratio R	0.00	0.25	0.50	0.75	1.00	0.75	0.50	0.25	0.00	0.25	0.50	0.75	1.00
Stress Regime	Radial Extensive		Pure Extensive		Transtensive		Pure Strike-Slip		Transpressive		Pure compressive		Radial compressive
Stress index R'	0.00	0.25	0.50	0.75	1.00	1.25	1.50	1.75	2.00	2.25	2.50	2.75	3.00
Determination of R'			R'=R				R'=2-R				R'=2+R		

4. Results

4.1. Petrography

Two petrographic units outcrop in the study area: the basement rocks and the sedimentary rocks (Fig. 3).

The basement outcrops in Pitoa and includes two petrographic types: the gneiss and the granite. The contact between sedimentary rock and bedrock is clearly observed in the field in this region (Figs. 3a, 3b). Gneisses are characterized by an alternation of quartz-feldspar rich clear and ferromagnesian rich dark bands (Fig. 3b). Granites are leucocratic and exhibit minerals such as quartz, k-feldspars, plagioclase and muscovite (Fig 3a).

Sedimentary rocks consist of conglomerates, coarse microconglomeratic sandstone, coarse sandstone, fine sandstone, siltstone and argillite. Conglomerates is reddish, whitish or greyish color and consist of sub-rounded pebbles, quartz joints and fragments of pink granite united by a silico-clay cement (Fig. 3j). It is predominantly made up of 1 - 2 mm size grains particles and display oblique stratifications. Conglomerates are surmounted by coarse microconglomeratic sandstone which are characterized by rounded shape pebbles, most of them being quartz particles and fragments of pink granite with a carbonate or clayey-sandy matrix. They contain oblique and cross stratifications (Figs. 3c, 3d, 3n). Sandstone constitutes the most abundant facies and present oblique stratifications and parallel laminations. They display three microfacies: coarse, motley, fine and reddish in color. Coarse sandstone, reddish or motley red to purple are composed of 1-2 mm size particles bounded by a silico-clay cement (Fig. 3l, n). Fine sandstone contains very fine particles (0.063 -1 mm) and are laminated (Fig. 3g). Siltone consists of 0.004 -0.063 mm size particles with a clay matrix and display red to purple color (Fig. 3k, l). Argillite is red to purple and is made up of less than 0.004 mm size particles (Fig. 3l, m).

These deposits are generally organized in prograding genetic parasequences, of variable thickness limited by flooding surfaces and refer to a fluvial palaeoenvironment marked by medium to high hydrodynamics, decreasing from base to summit.

4.2. Tectonic analysis

The structural elements collected from the Garoua basin are essentially brittle consisting of joints and faults. We used the term tectonic joint consistently to indicate a break in a rock where the orthogonal opening is predominant. On the contrary, if clear lateral displacement by shearing is observed, then we adopt the term fault.

4.2.1. Tectonic joints

Tectonic joints were observed mostly in sandstone and conglomerate. They are millimetric, rarely centimetric or decimetric and form planes that cross cut these rocks mostly intersect each other, forming simple or conjugate joint. Conjugated joints showing clear planes, were used to determine the spatial distribution of the paleostresses. In the study area, two types of joints were observed: dry tectonic joints f(Fig. 4 a, b, c) and filled joints containing quartz or other crystallized minerals (Fig. 4d). Most of these joints show complexes movements and then correspond to strike slip faults or shears.

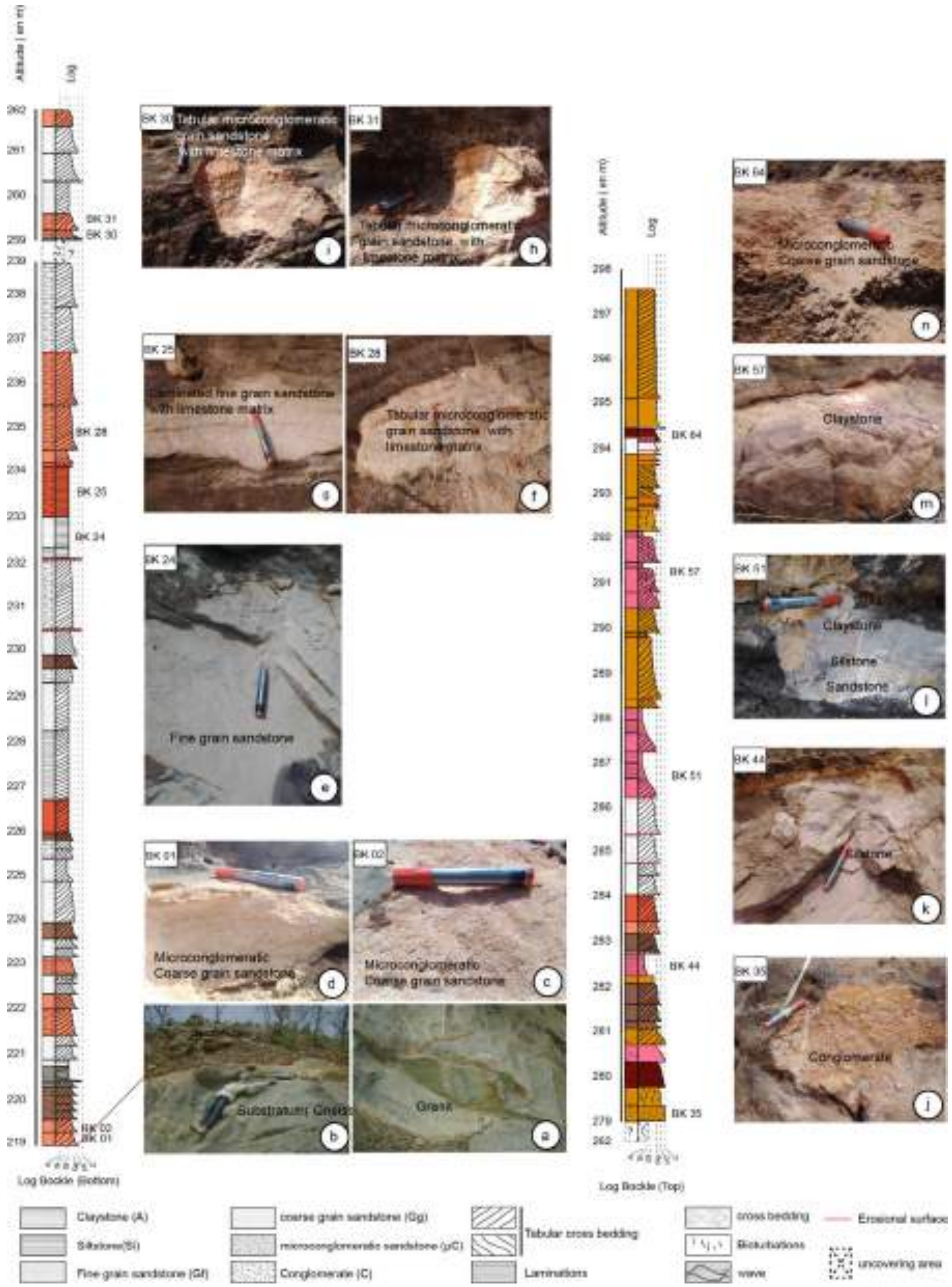

Fig. 3. Petrographic units outcroping study area and associated lithological logs. **(a)** Granit; (**b)** Gneiss; **(c**, **d, n)** Microconglomeratic coarse sandstone; **(e)** Fine grain sandstone; (**f, h, I)** Tabular microconglomeratic sandstone; **(g)** Laminated fine grain sandstone; **(J)** Conglomerate; **(k)** Silstone; **(l)** Sandstone, siltstone and claystone and **(m)** Claystone.

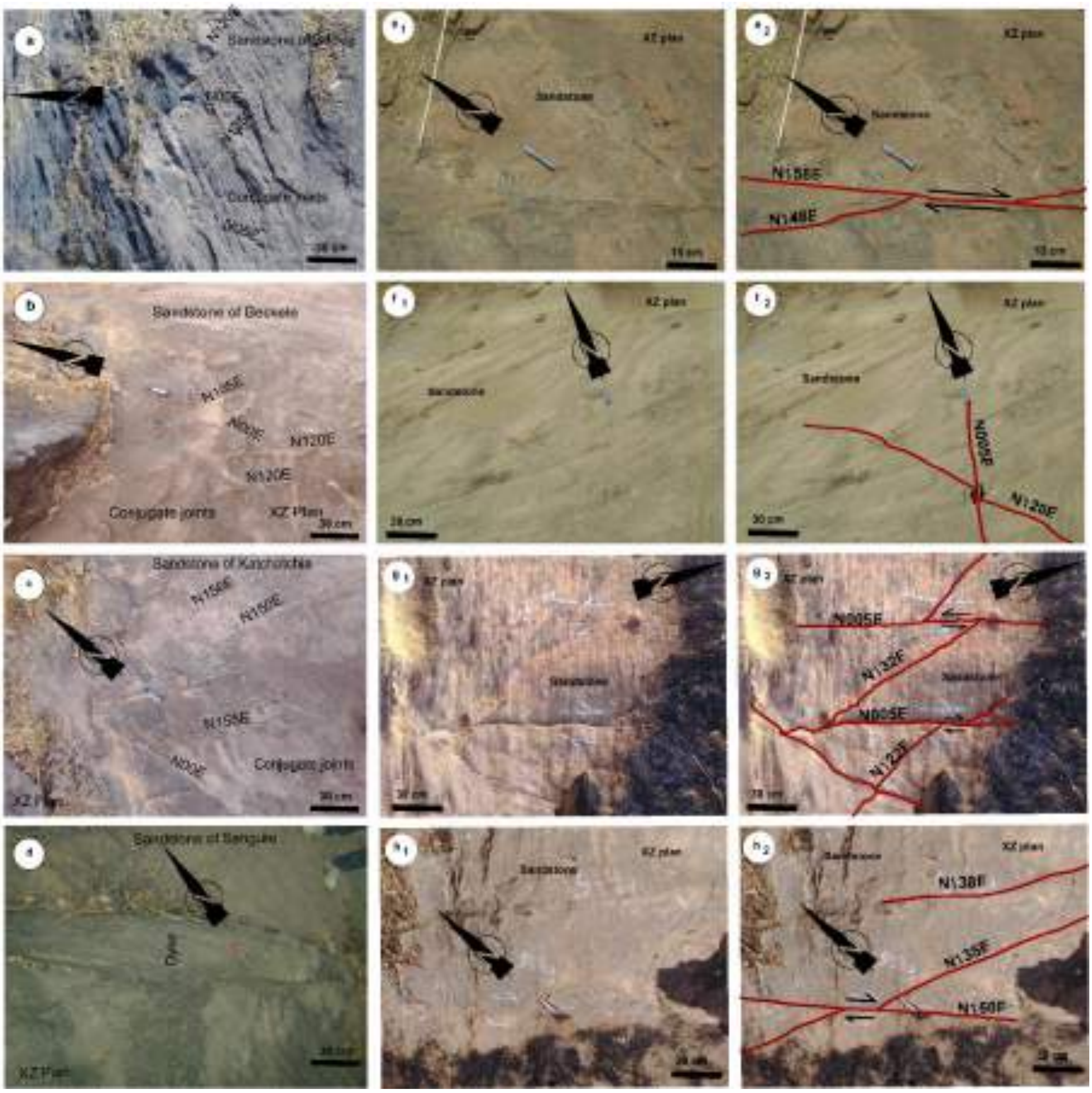

Fig. 4. Field photographs showing some structural features. **(a, b, c)** dry joints filled Joints; **(d)** filled joints; **(e, f, h)** dextral shear zone derived from joints displacements; **(g)** dextral and sinistral shear zone movement occurring during joints displacements.

4.2.1. Tectonic joints

Tectonic joints were observed mostly in sandstone and conglomerate. They are millimetric, rarely centimetric or decimetric and form planes that cross cut these rocks mostly intersect each other, forming simple or conjugate joint. Conjugated joints showing clear planes, were used to determine the spatial distribution of the paleostresses. In the study area, two types of joints were observed: dry tectonic joints f(Fig. 4 a, b, c) and filled joints containing quartz or other crystallized minerals (Fig. 4d). Most of these joints show complexes movements and then correspond to strike slip faults or shears.

- *Filled joints*

Rose diagrams and stereograms from these joints highlight a dominant NW-SE direction, followed by a N-S direction (Figs. 5A, 5B; Table 2). The average attitudes of these joints as well as stress directions vary from one station to another. These structures are associated with the extension and compression domains that slightly vary from site to site. The mean directions of extension and compression in the study area are NE-SW and NW-SE respectively (Figs. 5B, 5C).

In Beckele's locality, the main stress directions of σ_1 and σ_3 are NE-SW and NW-SE respectively with low plunges while σ_2, oriented NNW SSE is subvertical. σ1 (NW-SE) and σ3 (NE-SW) show very moderate to gentle plunges while, σ2 (NNW-SSE) has steep plunge in Katchatchia(Fig. 7b; Table 2). In Bockle, σ1 and σ3 are oriented NW-SE and NE-SW, with gentle plunges while σ2 is subvertical. The stereonet for the whole study area display an average attitude of N142E87NE with σ_1, σ_2 and σ_3 oriented NW-SE, NNW-SSE and NE-SW respectively (Table 2). R varies from 0.83 to 1 with a mean value of 0.63 and R' from 1 to 1.17 with the mean value of 1.09 (Table 2).

Table 2. Characteristic of joints and faults

Tectonic markers	Stations	Mean attitudes	Mean directions of poles	Paleotresses σ 1	Paleotresses σ 2	Paleotresses σ 3	R	R'	Stress ellipsoid	Tectonic regime
Filled joints	S2	N58E84SE	N148E10ENW	N57E2NE	N160E83SSE	N148E7NW	0.83	1.17	Triaxial	Transtensive
	S4	N135E84ESW	N70E8NE	N134E14NW	N152E76SSE	N45E4NE	1	1	Oblate	Transtensive
	S5	N141E88NE	N72E14WSW	N143E3NW	N151E87SSE	N53E00	0.9	1.1	Triaxial	Transtensive
	S	**N142E87NE**	**N70E11WSW**	**N141E5NW**	**N153E85SSE**	**N51E1NE**	**0.63**	**1.37**	**Triaxial**	**Pure strike slip**
Dry joints	S2	N118E77SSW	N28E13NNE	N123E18ESE	N79E66WSW	N28E16NNE	0.06	1.94	Triaxial	Transpressive regime
	S3	N117E89NNE	N39E1SW	N117E1ESE	N91E89W	N26E00	1	1	Oblate	Transtensive
	S4	N145E90	N55E00	N145E00	N139E90	N55E00	1	1	Oblate	Transtensive
	S5	N155E90	N65E00	N155E00	N22E90	N65E00	1	1	Oblate	Transtensive
	S	**N151E90**	**N63E00**	**N151E00**	**N24E90**	**N62E00**	**0.9**	**1.1**	**Triaxial**	**Transtensive**
Faults	S1	N129E86SW	N52E4NE	N128E1WNW	N54E86NE	N38E4SW	0.7	0.7	Triaxial	Pure extensive
	S2	N127E80 SW	N68E10ENE	N129E00	N39E83NE	N40E8NE	0.2	0.2	Triaxial	Radial extensive
	S3	N147E79NE	N88E11W	N140E5SE	N124E85WNW	N50E2SW	0.99	0.99	Triaxial	Transtensive
	S4	N135E83NE	N69E7WSW	N134E13NW	N120E76SSE	N43E3SW	0.88	0.88	Triaxial	Transtensive
	S5	N140E76NE	N72E14WSW	N144E19NW	N147E71SE	N54E1NE	0.26	0.26	Triaxial	Pure extensive
	S	**N133E80NE**	**N67E10WSW**	**N135E7NW**	**N138E83SE**	**N45E00**	**0.09**	**0.09**	**Triaxial**	**Radial extensive**

S: Synthesis; R: Stress ration; R: Stress index; S1: Pitoa; S2: Beckele; S3: Sanguere; S4: Katchatchia; S5: Bockle

- *Dry Joints*

As filled joints, rose diagrams of the dry joints show two families of joints: the NW-SE and the N-S families with dip ranging from 77 to 90° (Fig. 6A; Table 2). Density diagrams and stereograms show quite similar directions of extension and compression from station to the other (Figs. 6B, 6C). The average direction of extension is ENE-WSW, that of compression being NNW-SSE. In Beckele, σ_1 is oriented ESE-WNW and σ_3 NNE-SSW, both having low plunges while σ_2, oriented ENE-WSW show a steep plunge (66°WSW). In Sanguere, Katchatchia and Bockle, σ_1 is oriented ENE-WSW, NW-SE and NNW-SSE respectively; σ_3 NNE-SSW, NE-SW and ENE-WSW respectively with nil (0°) plunges (Fig. 10b). σ_2 oriented E-W, NW-SE and NNE-SSW respectively is vertical. R varies from 0.06 to 1 with a mean value of 0.63 and R' from 1 to 1.94 with the mean value of 1.23 (Table 2).

As we said above, most of these tectonic joints (dry or filled) materialize zones of strike slip or shearing. The locality of Bockle is good example fot the occurrence of these features. Indeed, on outcrops of this locality, N148E joints displaced by N158E joints exhibit dextral movement (Fig. 4e). Figure 4f shows another example where N120E joints display clockwise displacement induced by N-S (N05E) planes. Still in this station, N132E joints display clockwise displacement induced by N-S (N005E) sinistral planes (Fig. 4g).

4.2.2. Faults

The study area is affected by normal and vertical faults. These faults occur in the field as brittle structures exhibiting rock body's displacement with mirrors displaying slickenside lineation which indicate the direction of movement. Figure 7 summarizes faulting in the study area. This activity is best illustrated in Bockle, where the sandstone are affected by vertical faults whose mirrors display slickenslide lineation plunging towards the SW (Fig. 7a) and in Beckele where a vertical fault of attitude N138E90 was observed (Fig. 7f).

Normal faults have a very significant strike slip component. The Slickenslide lineation plunge towards the SW or NE (Fig. 7b, c). The average fault attitude in Bockle is N140E76NE. In Beckele, the fault planes have an average attitude of N127E80SW. Slickenslide lineations plunge to the SW (Fig. 5d). In Pitoa, Sanguere and Katchatchia, the average attitudes of faults are N129E86SW, N147E79NE and N135E83NE respectively with Slickenslide lineations plunging towards the SW or the NE.

Rose diagrams show two major fracture directions: NW-SE and NNW-SSE (Fig. 8a; Table 2). Their dips are comprised between 76 and 80° (Fig 8b; Table 2). Density diagrams and stereograms show NE-SW extension and NW-SE compression (Figs. 8B, 8C). Unlike joints, fault poles are more or less arranged on the horizontal plane (Fig. 8D). The mean direction of σ1 is NW-SE, that of σ3, NE-SW while σ2 is oriented NW-SE. Plunges are very low for σ1 and σ3 and very important for σ2 (83°). R and R' vary from 0.2 to 0.99 with a mean value of 0.09 (Table 2).

5. Discussion

Field observations in the Garoua basin suggest complex relationships between brittle deformation (i.e. fractures and faults). In this section we discuss the tectonic regimes of occurrence of fractures, the kinematics and chronology of the deformation as well as the influence of the geological features.

5.1. Tectonic regimes

Brittle deformation in the Garoua basin are represented by joints and faults. Both dry and filled joints have similar planar attitudes with steep to almost subvertical dips. The paleostress analysis and the values obtained from stress ratio (R) and stress index (R') show that for the filled tectonic joints: σ2 is vertical, R varies from 0.83 to 1 with a mean value of 0.63 and R' from 1 to 1.17 with the mean value of 1.09. According to Delvaux et al. (1997) and Sanderson (1997), such values and the occurrence of σ2 at the vertical refer to triaxial ellipsoid and pure strike slip regime (Table 2).

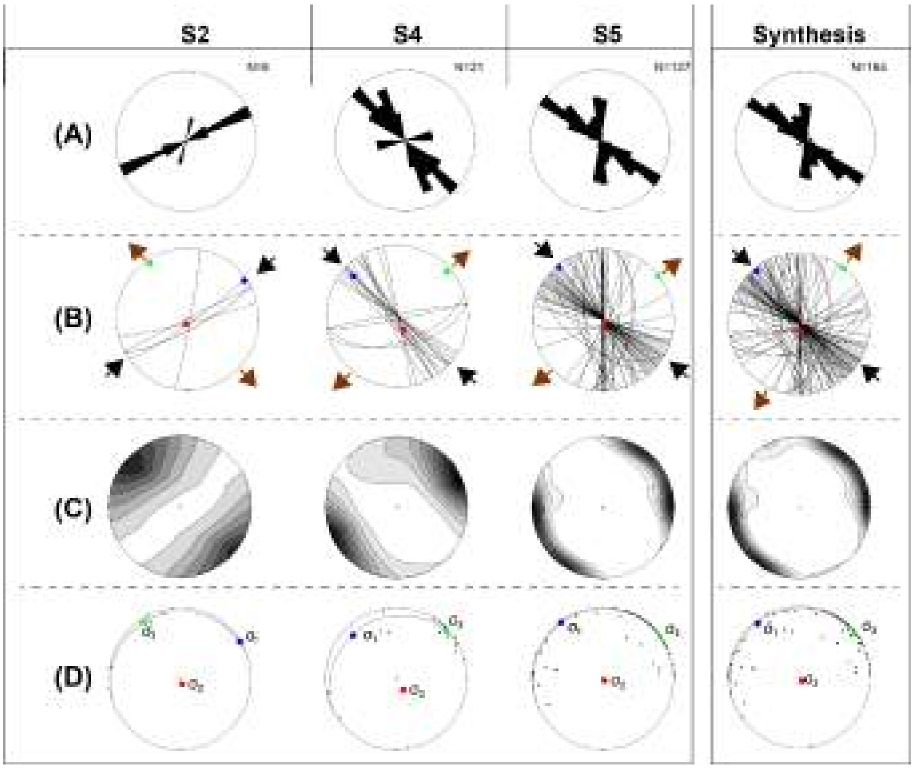

Fig. 5. Left panels: stereonet, lower hemisphere of (A) rose diagrams, (B) Stereograms, (D) density diagrams, contoured by using the Kamb exponential method and (D) poles diagrams to strike slip (filled joints with dextral pay). Right panels: synthesis of different diagrams. Mean values of stresses: σ1: N141E5NW; σ2: N153E85SSE; σ3: N51E1NE. Green points: σ3; bleu poins: σ2; and red points: σ1. S2: Beckele station; S4: Katchatchia station; S5: Bockle station.

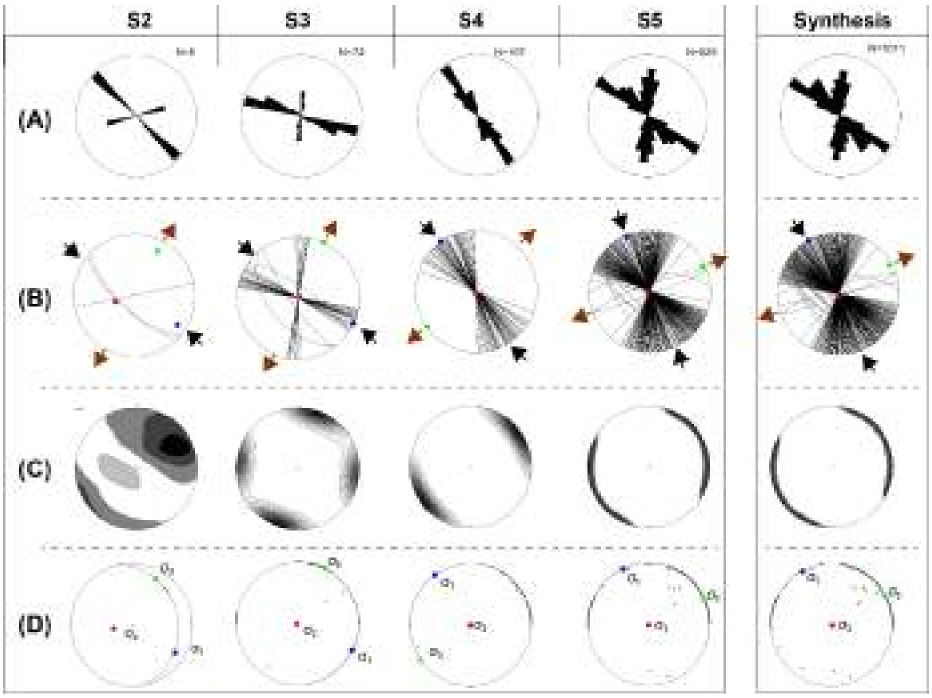

Fig. 6. *Left panels*: Stereonet, lower hemisphere of (A) rose diagrams, (B) Stereograms, (D) density diagrams, contoured by using the Kamb exponential method and (D) poles diagrams to strike slip (dry joints displaying dextral shear sense). *Right panels*: Synthesis of different diagrams. Mean values of stresses: **σ1**: N151E00; **σ2**: N24E90; **σ3**: N62E00. Green points: σ3; bleu poins: σ2; and red points: σ1. S2: Beckele station; S3: Sanguere station; S4: Katchatchia station; S5: Bockle station

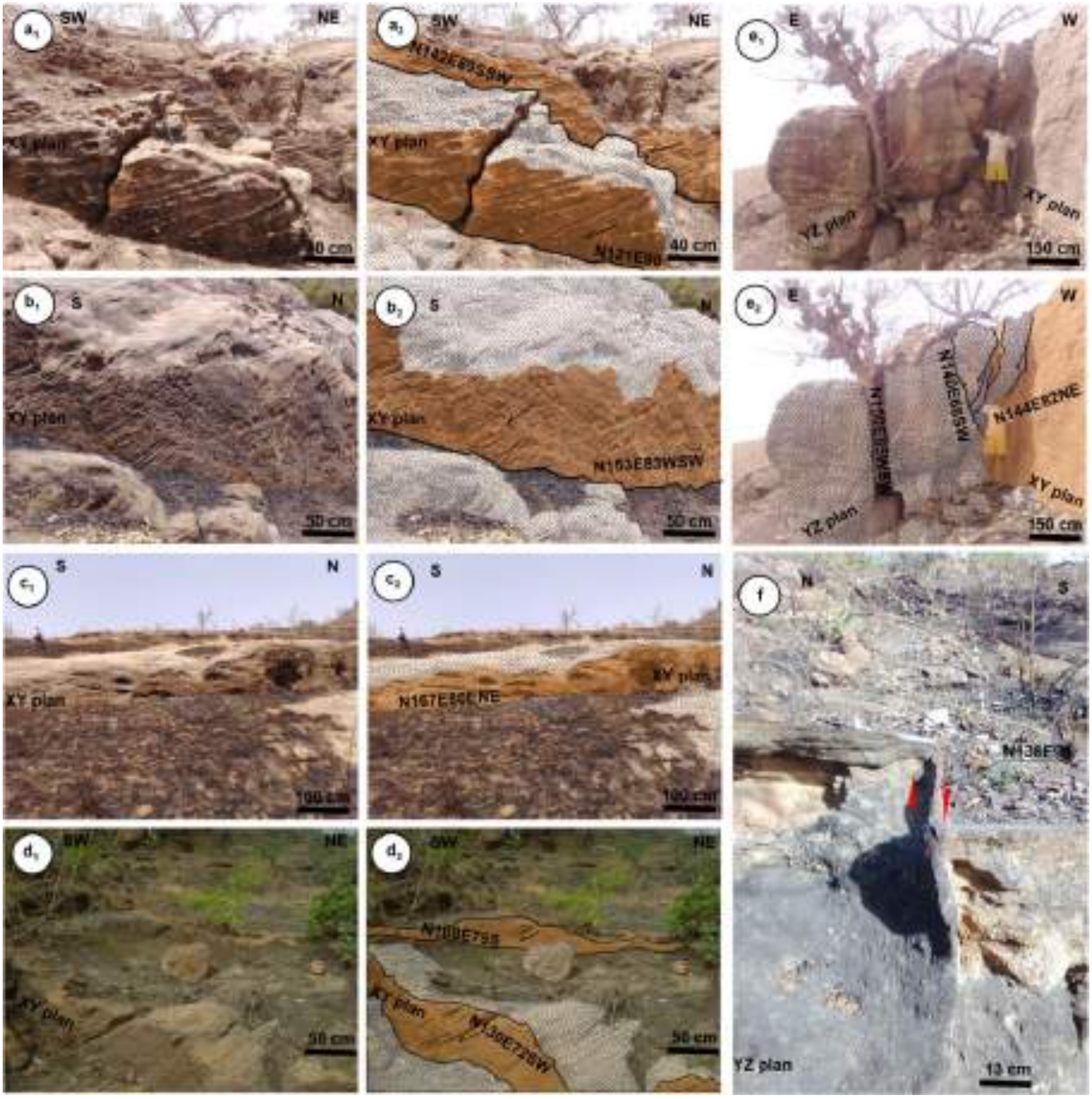

Fig. 7. Field photographs showing faults in the study area. (**a, b, d)** Faults planes showing slickenside lineation plunging towards the south; **(c)** Fault plane showing displacements of compartment to the North; **(e)** System of fractures showing opposite plunge (E and W); **(f)** Vertical fault.

For the dry joints, σ1 occurred at the vertical, R varies from 0.06 to 1 with a mean value of 0.63 and R' from 1 to 1.94 with the mean value of 1.23 for the dry tectonic joints referring to triaxial ellipsoid and pure extensive regime (Table 1).

As far as faults are concerned, R and R' vary from 0.2 to 0.99 with a mean value of 0.09 referring to triaxial ellipsoid and radial extensive regime (Table 1). Ultimately, it appears that, two tectonic regimes occurred in the Garoua basin: a strike slip and an extensive regimes. The compressive regime is weakly represented.

5.2. Chronlogy and kinematic

According to Maurin and Guiraud (1990), the Pan-African basement which shelters the Garoua basin was affected by four main directions of fractures: N-S, NW-SE, ENE- WSW and E-W to WNW-ESE. The N-S and E-W to WNW-ESE fractures occurred during the rifting that led to the formation of the Benue Through. These directions were well constrained in the Nigerian part of the Benue Through by Maurin and Guiraud (1990) and Benkhelil (2008). The Garoua basin itself also show four directions of fractures: NW-SE, N-S, ENE-WSW and NNW-SSE, with the first three similar to those encountered in the basement. This reflects probably a relationship between the basement and the sedimentary cover. It is therefore possible that faults recorded by the sedimentary rocks result from the reactivations of the basement faults. The second hypothesis is that these faults were set up during the replay of the main geological structures that cross or affect the basin i.e. LVC, BTJ and CCSZ. In the absence of seismic data enable to provide images highlighting the sediment bedrock relationships, we examined the action of regional structures.

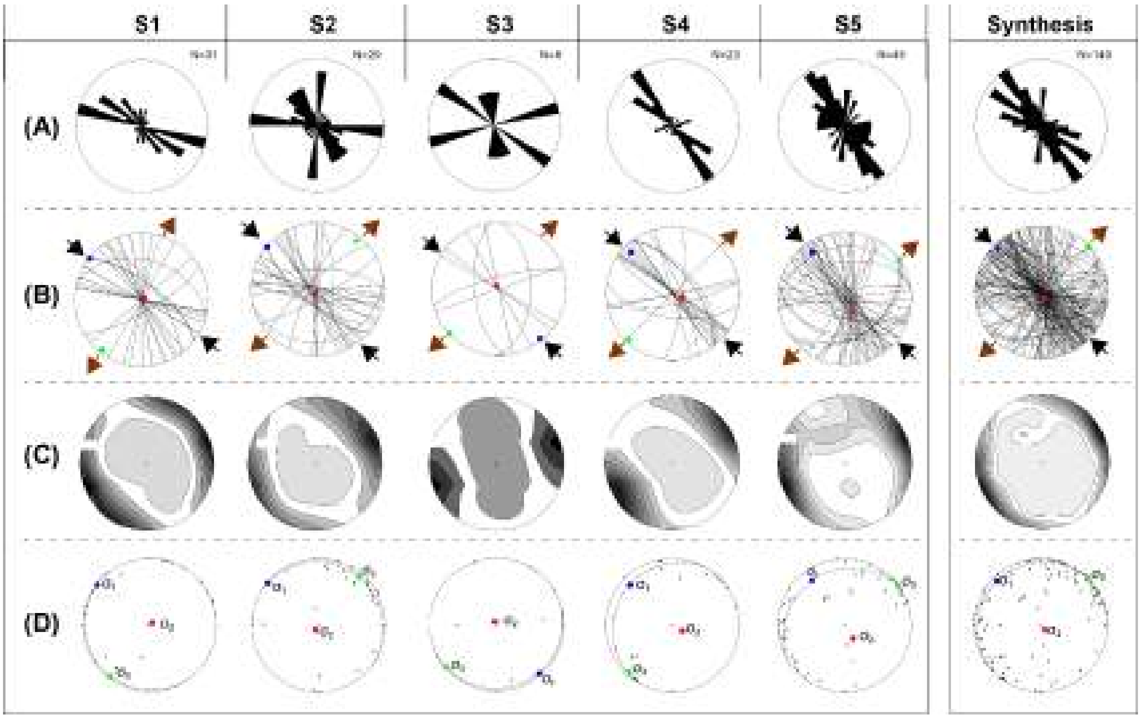

Fig. 8. *Left panels*: stereonet, lower hemisphere of (A) Rose diagrams, (B) Stereograms, (D) Density diagrams,contoured by using the Kamb exponential method and (D) Poles diagrams to faults. *Right panels*: Synthesis of different diagrams. Mean values of stresses: **σ1**: N135E7NW; **σ2**: N138E83SE; **σ3**: N45E00. Green points: σ3; bleu poins: σ2; and red points: σ1. S1: Pitoa station; S2: Beckele station; S3: Sanguere station; S4: Katchatchia station; S5: Bockle station.

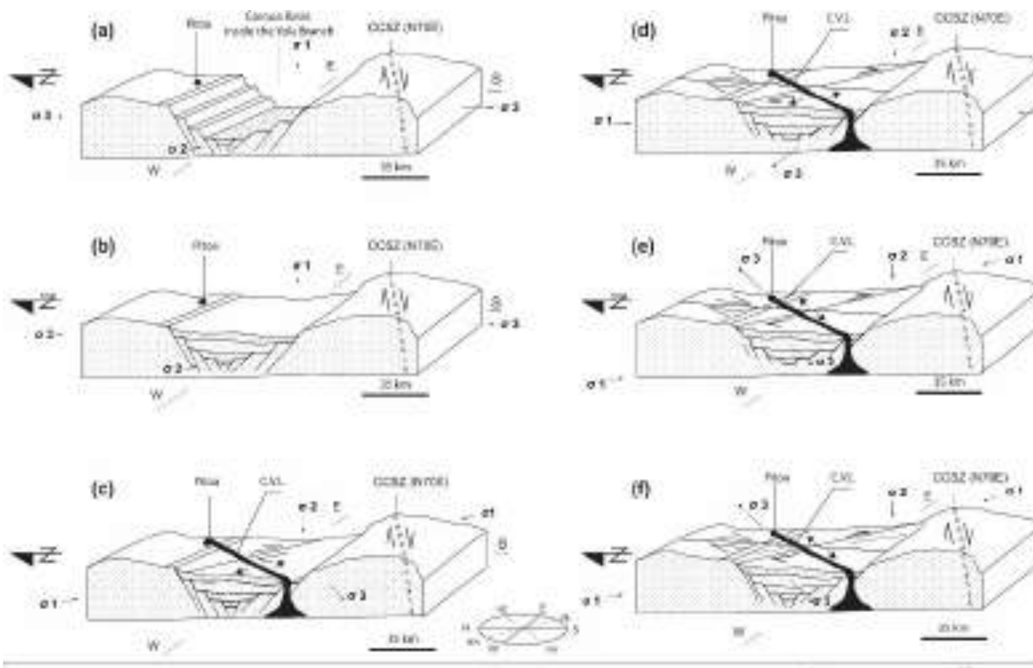

Fig. 9. Kinematic and evolution model of the Garoua basin from Aptian-Albian to Actual. **(a)** Aptian-Albian (rifting due to a N-S extension); **(b)** Albian to the Coniacian (basin filling); **(c)** Upper Eocene/Base Oligocene (occurrence of NW-SE dextral shears); **(d)** Upper Oligocene (occurrence of N-S strike slip faults); **(e)** Lower Miocene (implementation of NW-SE normal faults); **(f)** Messinian (formation of NNW-SSE normal faults).

Field data from Garoua basin reveal two major tectonic regimes: a strike slip regime marked mainly dextral and rarely sinistral shears in the NS and NW-SE directions and an extensive regime represented by normal faults in the NW-SE and NNW-SSE directions. The NW-SE dextral shears that affect the sediments seem to be post-sedimentary and earlier than the N-S joints. Indeed, the density diagrams and stereograms show that a NE-SW extension which affected these joints contributed to their filling. Research works from Wilson and Guiraud (1992), Fitton and Dunlop (1985), Ngounouno et al. (1993, 1997), Montigny et al. (2004) and Déruelle et al. (2007) have shown that the mounts Mandara (32 Ma) and the Benue Valleys (37 Ma), two volcanoes of the CVL aligned in a NE-SW direction are the only volcanoes that were active in the region. This activity which create an extension at this period must probably be at the origin of this fracture. We therefore propose an age at least equal to 37-32 Ma (Upper Eocene- Base Oligocene) for these fractures. The N-S system seems to be slightly younger since it intersects the NW-SE system with a dextral replay. It would probably be Upper Oligocene.
Faults also present two directions: the NW-SE and NNW-SSE directions. The first family is associated with a NE-SW extension phase clearly visible on density diagrams and stereograms. It corresponds to the direction of the upper border of the Yola Branch (Figs. 1b, 1c) and therefore, can be correlated to the reactivation in an extension regime during the Lower Miocene of the NE – SW rift system of the Benue Trough (Benkhelil 1988; Guiraud, 1991). The NNW-SSE faults, on the other hand, probably result from collapsing play of the N-S system (Ambraseys and Adams 1986; Ambeh et al., 1988).We can then conclude that joints were early and occurred following two directions: the NW-SE direction in the Eocene/Oligocene period and the N-S direction in the early Miocene.
A model of the evolution of the deformation was proposed (Fig. 9). This model contrasts with the classic model of deformation of the Barremo-Aptian basins of North Cameroon which indeed shows an extension in the N160E direction and a compression N70E (Maurin and Guiraud, 1990). Our model rather proposes an extension in the NE-SW direction and a compression in the NW-SE. The second essential difference is due the fact that the former model does take into account the reactivations of the BTJ which nevertheless significantly affected the basin. Finally our model has successfully integrated the BTJ and the CVL activities to reconstitute the chronology and the kinematic of the deformation in the Garoua basin.

Conclusion

The aim of this paper was to investigate the kinematics and the chronology of brittle deformation in the Garoua Basin. We focused our analysis on field surveys and literature data. Ultimately, it appears that, the Garoua basin was subjected in its post-rift phase to a progressive deformation of the brittle context with two main tectonic regimes: a strike slip regime and an extensive regimes.

The strike slip regime, early, was implemented into two phases: a NW-SE phase (Upper Eocene/base Oligocene) and the N-S (Upper Oligocene). The distensive regime also was deployed in two steps marked in the lower Miocene by the establishment of NW-SE normaj faults and in the Messinian by the occurrene of NNW-SSE normal faults. Then, the syn to post-rift history of the Garoua basin can be summarized into six main stages:

(a) during the Aptien-Albien, a N-S extension led to formation of the Benue Trough synchronously with that of Garoua basin;
(b) from the Albian to the Coniacian, the basin fill up;
(c) during the Eocene-Oligocene period, the first post-sedimentary NW-SE dextral shears controlled by the activity of the LVC occurred;
(d) during the late Oligocene / early Miocene, N-S strike slip faults with a dextral replay occurred;
(e) during the lower Miocene, NW-SE normal faults associated with a NE-SW and correlated with the reactivation in extension of the NE-SW rift system of the BTJ were set up;
(f) during the Messinian, the NNW-SSE normal faults due to the Collapsing play of the N-S system of the BTJ were formed.

The CVL and the BTJ were the main regional structures that controlled this evolution.

Acknowledgments

We thank the reviewers for their insightful, pertinent and useful comments. Special thanks go to Editor of this journal for its constructive suggestions to make the paper better.

References

Abubakar, M.B. 2006. Biostartigraphy, Paleoenvironments and Organic geochemistry of the Cretaceous sequences of Gongola Basin, Upper Benue Trough. PhD unpublished thesis, Abakar Balewa University, Nigeria. 315p.

Ambeh, B.W., Fairhead, J.D., and Stuart, G.W. 1988. Seismicity, structure and tectonics of the Cameroon Volcanic Line. Publication University of Leeds, Department of Earth Sciences, UK

Ambraseys, N.M., and Adams, R.D. 1986. Seismicity of West Africa. Ann. Geophys., 4:679–702.

Angeler, J. 1984. Tectonic analysis of fault slip data sets, Journal of Geophysical Research, (89):5835-5848.

Angeler, J.1990. Inversion of field data in fault tectonics to obtain the regional stress-III. A new rapid direct inversion method by analytical means. Geophysical Journal International, (103):363-376.

Arthaud, F. 1969. Méthode de détermination graphique des directions principales de raccourcissement, d'allongement et intermédiaire d'une population des failles. Bulletin de la société géologique de France, (11): 729-737.

Bao, H., Yong, Z., Hengzing, L., Kele, Z.Q.Qi., and Changgen, Y. 2019. Distribution characteristics and controlling factors of vertical joint spacing in sand-mud interbedded strata. Journal of Structural. Geology, (128):103886.

Benhkelil, J. 1982. Benue Trough and Benue chain: Geological Magazine, (119):155-168.

Benhkelil, J.1988. Structure et évolution géodynamique du basin intracontinental de la Bénoué (Nigéria): Société Nationale Elf-Aquitaine, Pau, France, 12: 29-128.

Bessong, M. 2012. Paléoenvironnements et Diagenèse dans un réservoir gréseux d'âge Crétacé du Fossé de la Benoué au Nord Cameroun : les grès de Garoua. Thèse de Doc Ph.D.Sci. Fond. et Appli. Terre solide et enveloppes superficielles. 196 p.

Bessong, M., Abderazack, E. A., Hell, J.V., Claude, F., Ndjeng, E., and Ngos III, S. 2011. Diagenesis in cretaceaous formations of Benue Trough in the Northern part of Cameroon Garoua sandstones world. Journal of engineering and pure and applied sci., 1(3):58.

Bessong, M., Hell, J., Elias, S., Suzanne, F.B., Ngos III, S., Eyong, J.T., Nolla, J.D., Mbesse, C.O., Thierry Adatte, Mfoumbeng, M.P., Dissombo, E.A., Ntsama, A.J., Mouloud, B., and Njeng, E. 2018. Hydrocarbon potential, palynology, palynofacies of four sedimentary basins, in the Benue Through, northern Cameroon. Journal of Earth Sci., 23p.

Bessong, M., Mbesse, C, O., Ntsama, A.J., Hell, J.V., Abderazack, E. A., Claude, F., Nolla, J.D., Dissombo, E., Eyong, J, T, and Mvondo, O, F. 2015. Mineralogy and clays minerals distribution in the Benue Trough, northern Cameroon (W.Africa): Diagenetic significance. International journal of applied research, 1(11):01-08.

Bisso, D., Mbida, Y., Koah Na Lebogo, S.P., Mvondo, O.J., and Tsoungui, C. 2016. Morphostructures et tectonique récente dans le bassin de Garoua Nord Cameroun. Afrique Science, 12(5) : 112-117.

Carey, E., and Brunier, B. 1974. Analyse théorique et numérique d'un modèle mécanique élémentaire appliqué à l'étude d'une population de failles. Comptes Rendus de l'Académie des Sciences, Paris, 279 (D): 891-894.

Carey, E., and Brunier, B. 1974. Analyse théorique et numérique d'un modèle mécanique élémentaire appliqué à l'étude d'une population de failles. Comptes Rendus de l'Académie des Sciences, Paris, 279 (D): 891-894.

Cornen, G.G., and Maury, R. C. 1980. Petrology of the volcanic island of Annobon, Gulf of Guinea. Mar. Geol., (25):253-267.

Daouda Dawaï. 2014. Les plutons de Guider et Bossoum-Pologozom (chaine panafricaine au Nord-Cameroun) : analyses pétrographique, structurale, magnétique, géochronologique et implications géodynamiques. Thèse Doc. Ph.D. Univ. Paul Sabatier-Toulouse III, 261p.

Delvaux, D., Moeys, R., Stapel, G., Petite, C., Levi, K., Miroshnichenko, A., Ruzhich, V., and San'kov, V. 1997. Paleostress reconstructions and geodynamics of the Baikal region, Central Asia, Part 2. Cenozoic rifting. Tcctonopliysics, (282):1-38.

Déruelle, B., Ngounouno, I., and Demaiffe, D. 2007. The Cameroon hot line (CHL): A unique example of active alkaline intraplate structure in both oceanic and continental lithospheres. Comptes Rendus Geoscience, (339):589-600.

rifts of Western end central Africa: an overview. Tectonophysics, 213:153-168.

Guiraud, R., Bellion, Y., Benkhelil, J., and Moreau, C.1987. Post-Hercynian tectonics in Northern and Western Africa. In: P. Bowden and J. Kinnaird (Editors), African Geology Reviews. Geol. J., 22: 433-466.

Guiraud, R., Bosworth, W., Thierry, J., and Delplanque, A. 2005. Phanerozoic geological evolution of Northern and Central Africa: an overview. Journal of African Earth Sciences, 43(1):83-143.

Han Bao, Yong, Z., Hengzing, L., Kele, Z.Q.Qi., and Changgen, Y. 2019. Distribution characteristics and controlling factors of vertical joint spacing in sand-mud interbedded strata. Journal of Structural Geology, 128:103886.

Homewood, P., Guillocheau, F., Eschard, R., and Cross, T.A. 1992. Correlations haute resolution et stratigraphie génétique: une démarche intégrée. Bulletin des centres de recherches exploration-Production Elf-Aquitaine, 16 : 203.

Jing Ye. 2016. Evolution topographique, Tectonique et sédimentaire Syn à Post-rift de la marge transformante Ouest africaine. Thèse Doc. Ph.D. Univ. Toulouse III Paul Sabatier, 275p.

Jolly, R.J.H., and Sanderson, D, J. 1997. A Mohr circle contruction for opening of pe-existing fracture. Journal of structural Geology, 19: 887-892.

Kamdem, J.B., Kraml, M., Keller, J., and Henjes-Krust, F. 2002. Cameroon line magmatism: conventional K/Ar and single-crystal laser 40Ar/39Ar ages of rocks and minerals from Hossere Nigo anorogenic complex Cameroon. Journal of African Earth Sciences, 35:99–105.

Kamgang P, Chazot G, Njonfang E, and Tchoua, F. 2008. Geochemistry and geochronology of mafic rocks from Bamenda Moutains (Cameroon): source composition and crustal contamination along the Cameroon volcanic line. CR Geosci., 340:850–857.

Koum, S., Mvondo Owono, F., Ntamack-Nida, M.J., Njom, B., and Belinga Essam, B.R. 2013. Surrection relative Plio-Pléistocène de la surface côtière de la marge sud du Rio del Rey (Cameroun) à partir de la géomorphologie quantitative sur Modèle Numérique de Terrain (MNT). Sc. Tech. Dév., 14: 59-60.

Kwekam, M., Légeois, J.P., Njonfang, E., Affaton, P., Hartmann, G., and Tchoua, F. 2010. Nature, origin and significance of the Pan-African high-K calc-alkaline Fomepea plutonic complex in the Central African Belt (Cameroon). Journal of African Earth Sciences, 57: 79-95.

Dumont, J.F.1987. Etude structurale des bordures nord de l'Adamaoua : influence du contexte atlantique. Geodynamique, 2(1):55-68

Etchecopar, A., Vasseur,G., and Daignières, M. 1981. An inverse problem in microtectonics for the determination of stress tensors form faults striation analysis. Journal of Structural. Geology, 3: 51-65

Faure, S. 1995. Reconstruction des paleocontraintes tectoniques dans les basses-terres du Saint-Laurent et les Appalaches du Québec et du nord du Nouveau-Brunswick. Thèse de Doctorat en Sciences de la Terre, 252p.

Fitton, J.G., and Dunlop, H.M. 1985. The Cameroon Line, West Africa, and its bearing on the origin of oceanic and continental alkali basalt. Earth Planet. Sci.Lett., 72:23-38.

Guiraud, M. 1991. Mécanisme de formation du basin crétacé sur décrochements multiples de la Haute Bénoué (Nigéria). Bulletin des centres de recherches exploration Production Elf Aquitaine, 15(1):11–67.

Guiraud, R., and Maurin, J.C.1991. Early Cretaceaous

Maurin, J., Benkhelil, J., and Robineau, B.1986. Wrench tectonics in Upper Benue, NE Nigeria ; Influence on the gepdynamics of the Cretaceous Benue Trough. 13ème Colloque de la Geologie africaine, ST Andrews, 199p.

Maurin, J.C., and Guiraud, R .1990. Relationships between tectonics and sedimentation in the Barremo-Aptian intracontinental Basins of Northern Cameroon. Journal of African Earth Sciences, 10: 331-340.

Moudi, A., Wandji, P., Bardintzeff, J-M., Ménard, J-J., Okomo Atouba, L.C., Reusser, E., Bellon, H., Tchoua, M.F. 2007. Les basaltes éocènes à affinité transitionnelle du plateau Bamoun, témoins d'un réservoir mantellique enrichi sous la ligne volcanique du Cameroun. CR Geosci. 339:396–406.

Mvondo Owono., F. 2001. Nouvelle approche de la déformation progressive du contexte fragile de Yaoundé et ses environs. Mémoire de DEA, Université de Yaoundé I, 50 p.

Ngako, V., Jegouzo, P., and Nzenti, J.P. 1991. Le Cisaillement Centre Camerounais. Rôle structural et géodynamique dans l'orogenèse panafricaine. CR Acad Sci Paris, 313(2):457–463.

Ngako, V., Affaton, P., Nnange, J.M., and Njanko, T. 2003. Pan-African tectonic evolution in central and southern Cameroon: transpression and transtension during sinistral shear movements. Journal of African Earth Sciences, 36:207–214.

Ngounouno, I. 1993. Pétrologie du magma ligne cénozoïque de la vallée de la Bénoué et du plateau de Kapsiki (Nord Cameroun). Thèse Doc. Univ. Pierre et Marie Curie, Paris-France, 280p.

Ngounouno, I., Nkoumbou, C., and Loule, J.P.1997. Relations entre l'évolution tectono-sédimentaire et le magmatisme du Fossé de Garoua (nord-Cameroun). Africa Geoscience review, 4(3/4):451-460.

Nkouathio, D.G., Kagou Dongmo, A., Bardintzeff, J.-M., Wandji, P., Bellon, H., and Pouclet, A. 2008. Evolution of volcanism in graben and horst structures along the Cenozoic Cameroon Line (Africa): implications for tectonic evolution and mantle source composition. Mineral Petrol., 94:287–303.

Ntsama, A.J. 2013. Magnétostragraphie et sédiimentologique des formations crétacées des bassins sédimentaires d'Hamakoussou et du Mayo Oulo-Léré au Nord-Cameroun (Fossé de la Bénoué). Thèse Doc. Ph.D. Univ. Poitiers-France, 193p.

Nzenti, J.P., Barbey, P., Macaudière, J., and Soba, D. 1988. Origin and evolution of the late Precambrian high - grade Yaoundé gneisses (Cameroon). Precambrian Research, 38: 91 - 109.

Owona, S., Mbola Ndzana, S.P., Mvondo Ondoa, J., Nsangou Ngapna, M., NKabsaah, C., Ratschbacher, L., and Ekodeck, G.E., 2012. Geological control of morphotectonic units in the southwest Cameroon (central Africa). Journal of Geology and Mining Research, 4 (7):152 - 167.

Popoff, M.1988. Du Gondwana à l'Atlantique sud : les connexions du fossé de la Bénoué avec les bassins du Nord-Est brésilien jusqu'à l'ouverture du Golfe de Guinée au Crétacé inférieur : Journal of African Earth Sciences, 7 : 409-431.

Sanderson, D.J., Peacock, D.C.P., Nixon, C.W., and Rotevatn, A. 2018. Graph theory and the analysis of fracture networks. Journal of Structural Geology, 29p. Doi:10.1016/j.jsg.2018.04.011.

Sarki Yandoka, M. B., Abdullah, W. H., and Abubakar. M.B., 2014. Geochemical characterisation of Early lacustrine sediments of Bima formation, Yola sub-basin, Northern Benue Trough, NE Nigeria: Organic matter input, preservation, paleoenvironment and paleoclimatic conditions. Marine and Petroleum Geology, 61: 82-94.

Tchaptchet Tchato, D., Schulz, B., and Nzenti, J.P., 2009. Electron microprobe dating and thermobarometry of Neoproterozoic metamorphic events in Kekem area, Central African fold Belt of Camroon. Stuttgard, 186: 95-109.

Tcheumenak, K.J., Njanko, T., Kwékam, M., Naba, S., Bella Nké, E.B., Yakeu Sandjo, A.F., Fozing, E.M., and Njongfang, E. 2014. Kinematic evolution of Fodjomewet-Fotoumi shear zone (West-Cameroon): Implications for emplacement of the Fomopéa and Bandja plutons. Journal of African Earth Sciences 99: 261-275.

Tiessen, B., Burke, K.C., and Kidd, W.S.F.1979. African hotspots and their relation to the underlying mantle. Geology, 7:263-266.

Toteu, S.F., Michard, A., Bertrand, J.M., and Rocci, G. 1987. U-Pb dating of Precambrian rocks from Northern Cameroon, orogenic evolution and chronology of Pan-African belt of Central Africa. Precambrian Research, 37:71-87.

Toteu, S.F., Penaye, J., and Djomani, Y.H.P. 2004. Geodynamic evolution of the Pan-African belt in Cenral. Canadian Journal of Earth Sciences, 41**:** 73–85.

Toteu, S.F.1990. Geochemical characterisation of the main petrographical and structural units of Northern Cameroon; implications for the Pan-African evolution. Journal of African Earth Sciences, 10:615-624.

Untemehr, P., and Bouche, P. 1986. South Atlantic opening: structural geological constraints. In: Sager W, Scotese C (eds), mesozoic and cenozoic plate reconstructions geodyn symp (Texas A&M Univ, Austin, 1986) (Abstr)

Wilson, M., and Guiraud, R.1992. Mesozoic-Cenozoic magmatism associated with the West and Central African rift System. In: P.A. Ziegler (Editor), Geodynamics of rifting, Volume II. Case History studies on Rifts: North and South America and Africa. Tectonophysics, 213: 203-225.

Youri, H., and Merzeraud, G., 2005. Nouvelles données sur le Trias de Sologne : Chemery, sud-ouest du bassin de Paris : Stratigraphie et environnement de dépôts. Geologie de la France, pp. 3-22.

Zarboski, P.F., Ubgodulunwa, A., Idornigie, P., Nnabo, K., and Ibe.1997. Stratigraphy and structure of the Cretaceaous Gongola basin, Northwest Nigeria. Bull. Cent. Res. Explor. Prod. Elf Aquat., 21(1): 154-185.